FACTA UNIVERSITATIS
Series: **Automatic Control and Robotics** Vol. 13, N^{o} 1, 2014, pp. 1 - 14

Regular paper

NONLINEAR MOTION CONTROL OF HUMANOID ROBOT UPPER-BODY FOR MANIPULATION TASK*

UDC (681.518.52+621.391.823):006.06

Srđan Savić, Mirko Raković, Marko Penčić, Branislav Borovac

University of Novi Sad, Faculty of Technical Sciences, Novi Sad, Republic of Serbia

Abstract. *This paper presents nonlinear control algorithm for motion control of humanoid robot upper-body. Upper-body consists of two arms, each having seven degrees of freedom (DOFs), and multi-segment lumbar spine with six DOFs which enables motion of the trunk, increases the workspace of robot arms and contributes to anthropomorphic appearance of the robot movements. Manipulation task, where robot is supposed to move an object of unknown mass, in presence of parameter uncertainties and external disturbance has been considered. Weight of the object has been considered as an external disturbance. Nonlinearity of the robot dynamical model and coupling between robot segments have been taken into account during control design. Sliding mode control with disturbance estimator has been used in order to provide accurate trajectory tracking in presence of disturbances. Efficiency of the proposed control algorithm is verified through a numerical simulation and results are presented.*

Key words: *motion control, sliding mode, humanoid robot, robot spine, manipulation*

1. INTRODUCTION

Nowadays number of robots and their presence in human environment is constantly increasing. Modern industrial robots, like ABB dual arm concept *Frida*, have been designed to cooperate with humans in factories [1]. Significant results have been also achieved in fields of service robotics [2] and assistive technologies [3, 4]. In all these applications it is important to make robots safe for people in their surrounding and to provide design and functionality of robots that would make people feel comfortable in their presence. For

Received February 10, 2014
Corresponding author: Srđan Ž. Savić
Faculty of Technical Sciences, Trg Dositeja Obradovića 6, 21000 Novi Sad, Republic of Serbia
E-mail: savics@uns.ac.rs
* **Acknowledgement**: This work was funded by the Ministry of education and science of the Republic of Serbia under contract III44008 and by Provincial secretariat for science and technological development under contract 114-451-2116/2011. The authors are grateful to Dunkermotoren for support and motors donation.

successful human-robot cooperation it is necessary to fit robot design and its functionality into established human social frames and protocols. Robot prototype, presented in this paper, is being developed at the University of Novi Sad, Faculty of Technical Sciences, and it is conceived as a mobile platform for research of socially acceptable robot behavior. This research includes bilateral interaction between humans and robots, speech recognition and synthesis, gesticulation, emotion recognition and expression, and robot behavior in unstructured environment. The experiments including industrial robot (our humanoid is not manufactured yet), stereo vision system, and speech recognition and synthesis system integrated with cognitive dialog management system have already been realized [5]. Manipulation with various objects is one of the basic tasks for robots working in human's environment. Since human arms are among the most advanced manipulation systems in nature, they were used in our work as inspiration for mechanical design of robot arms. Therefore robot arm design with 7 DOFs, inspired by human arm anatomy, is proposed in this paper in order to make robot arm movements as much as possible efficient and similar to human arms movements.

There are a lot of successful realizations of anthropomorphic robot arms. Some state-of-the-art solutions can be seen in robots *DLR-Lightweight-Robot-III* [6], *ARMAR* [2] and *ROBONAUT* [7]. These robot arms are actuated with electrical DC motors and have anthropomorphic kinematic structure with 7 DOFs, which makes them kinematicaly redundant. In some solutions of robot arm design pneumatic actuators are used [8].

Most of humanoid robots are developed with rigid torso, which makes their movement unnatural and constrained [9]. There are only few realizations of flexible robot spines. Some of them are robots *KENTA* [9], *UCL* [10] and *KOTARO* [11]. These solutions are biologically inspired and copy the anatomy of human spine. Spines of these robots are tendon driven which makes them more compliant and increases safety in case of physical contact with humans. They also have very low backlash. Flexible spine is able to absorb mechanical shock or impact. Disadvantages of these solutions are lower accuracy and repeatability. Tendons are susceptible to stretching due to material aging and creep. This can badly affect system performances. Another common solution of robot spine design is based on 2 DOFs tendon driven differential drive. This design can be seen in robots *iCUB* [12] and *ARMAR* [13]. It is very compact and has high stiffness and accuracy. Since the whole trunk motion is realized in a single joint it does not look natural and anthropomorphic.

In this paper a lumbar spine structure with 6 DOFs, proposed in [14], will be used. Spine consists of three serially connected segments, each having 2 DOFs, rotation and lateral flexion. Such movable spine structure increases workspace of robot arms and significantly contributes to anthropomorphic appearance of robot upper-body motion.

Since every model is only an approximation of a real system it is expected that the real robot will have slightly different parameters compared with corresponding CAD model. Besides parameters uncertainties robot will be exposed to external disturbances caused by collisions or unknown payload masses. Therefore it is necessary to design control algorithm which is robust to parameter uncertainties and disturbances and which is capable of achieving accurate trajectory tracking. A lot of papers have already been written on robust control of robot manipulators. A survey on sliding mode control can be found in [15], [16].

Paper is organized as follows. Basic description of robot upper-body mechanical design is given in chapter 2. In chapter 3 kinematic and dynamic model of robot are presented. Proposed control algorithm and simulation results for manipulation task in presence of parameter uncertainties and external disturbance are shown in chapter 4 and 5, respectively.

2. Mechanical Design of Spine and Arms

Mechanical design of biologically inspired anthropomorphic robot arms and multi-segment lumbar spine structure is described in this chapter. In Fig. 1 CAD model of robot upper-body is shown.

Kinematic structure with 7 DOFs, closely approximating human arm, has been adopted for robot arm. Shoulder has 3 DOFs (flexion/extension, abduction/ adduction, rotation) and consists of three revolute joints whose axes of rotation intersect in one point.

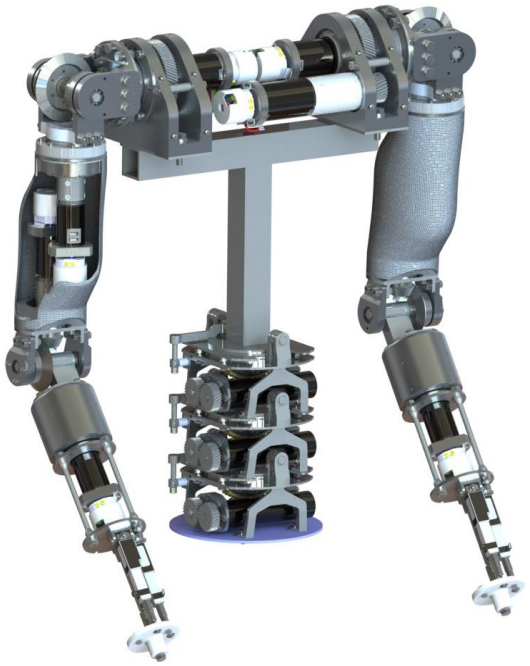

Fig. 1 CAD model of robot upper-body

All DOFs of shoulder are actuated with brushless DC motors (Dunkermotoren BG series motors), with integrated multi-turn digital absolute and incremental encoders to measure joint positions and velocities. Actuators for first and second DOF are placed in robot torso to reduce masses and moments of inertia of arm movable parts. Elbow joint has one DOF (flexion/extension) while wrist has 3 DOFs (rotation, flexion/extension and abduction/adduction) whose axes of rotation intersect in one point. Elbow flexion and wrist rotation are also actuated with Dunkermotoren brushless DC motors with integrated encoders, same as in the shoulder. Wrist flexion and abduction are actuated with linear actuators. Axes of rotation of these two DOFs intersect in the center of universal joint which is fixed on the central rod [17]. These linear actuators have integrated linear potentiometers for position measurement. Details about arm mechanical design and mechanical parameters can be found in [18].

Proposed lumbar spine design has three segments with 6 DOFs in total. This kinematic structure is able to realize movements of lateral flexion and rotation in each segment. Humans perform flexion/extension movements in hip up to 45°, not in spine.

Therefore implementation of this movement was not considered during design phase. For actuation of lateral flexion joints brushed DC motors are used. These motors have integrated planetary gear heads and incremental encoders for angle and angular velocity measurement. Power transfer from motor shaft to joint shaft is realized with spur and worm gears. Worm gears are used to achieve compact design and self-locking in any posture. Thus, increased reliability and preservation of upper body posture without additional energy has been achieved. For additional height reduction, specially profiled worm wheel has been designed. Torsion joints are realized as specially designed inseparable axial bearings. For actuation of torsion joints linear actuators are used. These actuators consist of DC motor with spindle drive and have embedded linear potentiometers. In Fig. 2 CAD model of robot lumbar spine is shown. Total height of three incorporated segments is 201 mm, diameter of the base is 150 mm, and the spine's mass is 6 kg (2 kg per segment). Total range of lateral flexion in three joints is ±30°, and total range of torsion in all joints is ±45°.

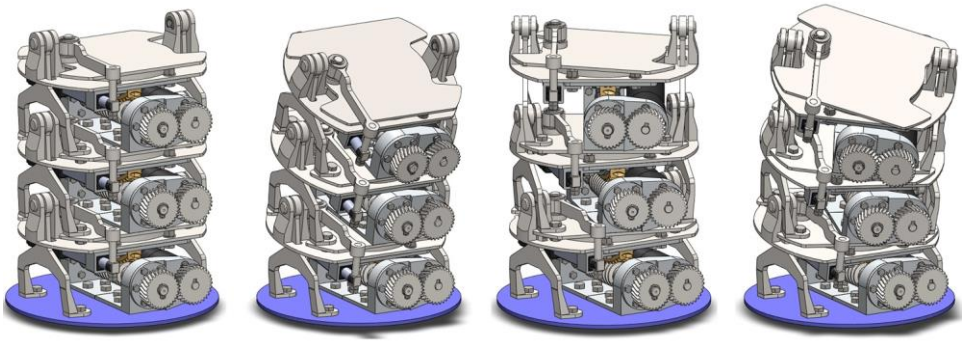

Fig. 2 The lumbar spine CAD model: (left) in initial upright position; (second from the left) lateral flexion (30°); (second from the right) torsion (45°); (right) flexion (30°) + torsion (45°)

3. KINEMATIC AND DYNAMIC MODEL

The robot upper-body used in this work is modeled in software that is capable of forming dynamic model of humanoid robots [19]. Software was developed at Faculty of Technical Sciences Novi Sad and it works in MATLAB environment. Both dynamics and control are simulated in this software which provides the possibility to simulate robots with one or more open and closed kinematic chains. Kinematic chains links are connected with simple joints having one rotational DOF. Robot kinematic model is shown in Fig. 3. Bottom segment of the spine is selected as a base link. State vector **q** consists of the position (x, y, z) and orientation of the base link (φ, θ, ψ) and the n-elements vector, consisting of relative angles between two adjacent links, where n represents the number of the mechanism links without base link. So, the total number of the mechanism DOFs is $6+n$:

$$\mathbf{q} = \left[x, y, z, f, q, y, q_1, q_2, \ldots, q_n\right]^T, \tag{1}$$

Kinematic model presented in Fig. 3, has two kinematic chains. The first chain comprises the spine and left arm and second the spine and right arm. Position and orientation of base link is constant, which means that the first 6 values in vector **q** are not changing.

To realize the motion of robot spine, the appropriate driving torques should be applied at each DOF. Since driving torques cannot be applied to the first 6 DOFs that determine the position and orientation of the basic link, the vector of driving torques is defined in the following way:

$$\boldsymbol{\tau} = \left[0,0,0,0,0,0,t_1,t_2,...,t_n\right]^T . \tag{2}$$

The dynamic model of humanoid robot is (in accordance with the defined vectors **q** and **τ**):

$$\boldsymbol{\tau} + \sum_{i \in P} \mathbf{J}_i^T \mathbf{F}_i = \mathbf{H}(\mathbf{q}) \cdot \ddot{\mathbf{q}} + \mathbf{h}_0(\mathbf{q}, \dot{\mathbf{q}}),\ \mathbf{h}_0(\mathbf{q}, \dot{\mathbf{q}}) = \mathbf{C}(\mathbf{q}, \dot{\mathbf{q}}) + \mathbf{G}(\mathbf{q}) , \tag{3}$$

where **τ** is vector of driving torques, **q** is vector of generalized coordinates, **H**(**q**) is symmetric, semi-definite inertia matrix, **C**(**q**, $\dot{\mathbf{q}}$) is vector of Coriolis and centrifugal moments, **J** is Jacobian matrix, **F** constant disturbance vector and **G**(**q**) is vector of gravitational moments. Each arm is modeled as a mechanism having 7 DOFs, spine is modeled as 6 DOF system, and the overall number of DOFs is 26 (additional 6 DOFs representing position and orientation of base link).

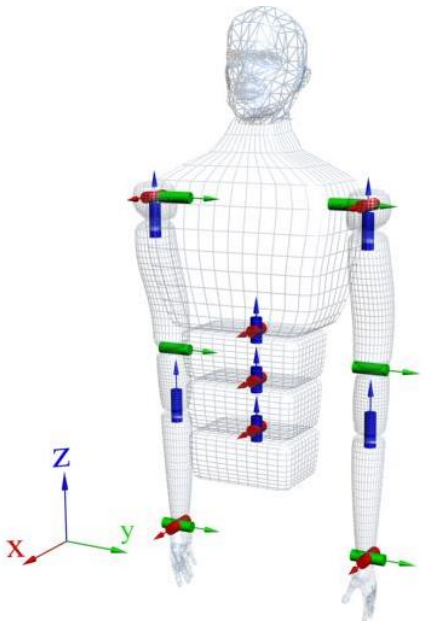

Fig. 3 Kinematic structure of the robot upper-body

4. CONTROL ALGORITHM

4.1. Feedback linearization

Humanoid robot modeled by (3) is multivariable, coupled and highly nonlinear system. In order to cancel system nonlinearities feedback linearization has been used. To apply feedback linearization it is convenient to represent robot dynamic equation (3) in the state space in controllability canonical form [15]:

$$\ddot{\mathbf{q}} = \mathbf{f}(\mathbf{q},\dot{\mathbf{q}}) + \mathbf{b}(\mathbf{q})\boldsymbol{\tau} + \mathbf{d} = -\mathbf{H}^{-1}(\mathbf{q})\mathbf{h}_0(\mathbf{q},\dot{\mathbf{q}}) + \mathbf{H}^{-1}(\mathbf{q})\boldsymbol{\tau} + \mathbf{H}^{-1}\sum_{i\in P}\mathbf{J}_i^T\mathbf{F}_i\,, \tag{4}$$

$$\mathbf{X} = \begin{bmatrix}\mathbf{q}\\ \dot{\mathbf{q}}\end{bmatrix},\ \frac{d}{dt}\mathbf{X} = \begin{bmatrix}\dot{\mathbf{q}}\\ \ddot{\mathbf{q}}\end{bmatrix} = \begin{bmatrix}\dot{\mathbf{q}}\\ \mathbf{f}(\mathbf{X}) + \mathbf{b}(\mathbf{X})\boldsymbol{\tau} + \mathbf{d}\end{bmatrix}, \tag{5}$$

where $\boldsymbol{\tau}$ is the vector of driving torques, $\mathbf{q}$ is output vector of joints angles, $\mathbf{X}$ is the state vector, $\mathbf{d} = \mathbf{H}^{-1}\sum_{i\in P}\mathbf{J}_i^T\mathbf{F}_i$ is the vector of joints accelerations caused by constant disturbance vectors $\mathbf{F}_i$, and $\mathbf{f}$ and $\mathbf{b}$ are nonlinear functions of states. Nonlinear dynamics $\mathbf{f}$ and control gain $\mathbf{b}$ are unknown but can be estimated based on the known model as $\hat{\mathbf{f}}$ and $\hat{\mathbf{b}}$.

To successfully control the motion of the robot by using feedback linearization method it is necessary that the system model is precise ($\hat{\mathbf{f}} = \mathbf{f}$, $\hat{\mathbf{b}} = \mathbf{b}$) and that there are no external disturbances ($\mathbf{F}_i = 0$). At this point it is assumed that this is true. Parameter uncertainties and external disturbances will be introduced in following subsections. By choosing control law in form:

$$\boldsymbol{\tau} = \mathbf{b}^{-1}(\mathbf{v} - \mathbf{f})\,, \tag{6}$$

nonlinearities are cancelled and the state space model (5) is reduced to a system of double integrators:

$$\ddot{\mathbf{q}} = \mathbf{v}\,. \tag{7}$$

Pole placement method is used to ensure desired dynamics of the system. If we consider a problem of trajectory tracking, by choosing $\mathbf{v}$ in the form:

$$\mathbf{v} = \ddot{\mathbf{q}}_\mathbf{d} - \mathbf{K}_1\dot{\mathbf{e}} - \mathbf{K}_0\mathbf{e}\,, \tag{8}$$

where $\mathbf{e}(t)$ is tracking error, exponentially convergent tracking is obtained [15]. Matrices $\mathbf{K}_1$ and $\mathbf{K}_0$ are diagonal Hurwitz gain matrices. Values for natural undamped frequency $\omega_0=10\pi$ and relative damping coefficient $\xi=1.5$ have been chosen and they define values of desired closed-loop poles s_1=-114.23 and s_2=-17.2864. Elements of matrices $\mathbf{K}_1$ and $\mathbf{K}_0$ are calculated as $k_1=2\xi\omega_0$ and $k_0=\omega_0^2$ to provide desired dynamic behavior of the system.

4.2. Sliding mode control

In reality model is never precise and it is only an approximation of a real system. Therefore it is necessary to modify control law to make it robust to parameter uncertainties and disturbances. In this paper it is done by using sliding mode control.

Time-varying hypersurface $\mathbf{S}(t,\mathbf{x})=0$ in state space is defined:

$$\mathbf{s} = \dot{\mathbf{e}} + \mathbf{\Lambda e} = 0\,, \tag{9}$$

where $\mathbf{\Lambda}$ is diagonal Hurwitz matrix. Elements λ of matrix $\mathbf{\Lambda}$ have been chosen to be equal with values of dominant pole s_2=-17.2864. Trajectory tracking problem can be considered as a problem of remaining on surface **S** during the motion. Control law:

$$\mathbf{u}_{eq} = \mathbf{v} - \mathbf{f} = \ddot{\mathbf{q}}_\mathbf{d} - \mathbf{K_1}\dot{\mathbf{e}} - \mathbf{K_0}\mathbf{e} - \mathbf{f}\,, \tag{10}$$

is equivalent continuous control that would keep system trajectory on hypersurface **S** ($\dot{\mathbf{s}} = 0$) if the system model were precise. In order to provide system stability in the sense of Lyapunov and exponentially convergent trajectory tracking so-called sliding condition has to be fulfilled. First Lyapunov-like function **V** is defined:

$$\mathbf{V} = \frac{1}{2}\mathbf{s}^T\mathbf{s} \geq 0\,. \tag{11}$$

Sliding condition is now given in the following form:

$$\dot{\mathbf{V}} = \frac{1}{2}\frac{d}{dt}\mathbf{s}^T\mathbf{s} = \mathbf{s}^T\dot{\mathbf{s}} \leq -\boldsymbol{\eta}|\mathbf{s}|\,, \tag{12}$$

where $\boldsymbol{\eta}$ is the vector of strictly positive constants that govern the reaching time. As already mentioned, unknown nonlinear dynamics **f** and control gain **b** from (4) can be estimated based on the known model as $\hat{\mathbf{f}}$ and $\hat{\mathbf{b}}$. It is assumed that estimation errors, as well as the value of external disturbance, are bounded by known functions **F**, $\boldsymbol{\beta}$ and **D**:

$$\left|\mathbf{f} - \hat{\mathbf{f}}\right| \leq \mathbf{F}(x, \dot{x}),\quad \left|\hat{\mathbf{b}}\mathbf{b}^{-1}\right| \leq \boldsymbol{\beta},\ \ |\mathbf{d}| \leq \mathbf{D}\,, \tag{13}$$

In our simulation values of **F**, $\boldsymbol{\beta}$ and **D** are calculated in the following way:

$$\mathbf{F}(x, \dot{x}) = \left|\mathbf{f} - \hat{\mathbf{f}}\right| = \left|\mathbf{H}^{-1}\mathbf{h_0} - \hat{\mathbf{H}}^{-1}\hat{\mathbf{h}}_\mathbf{0}\right|,\ \ \boldsymbol{\beta} = \left|\hat{\mathbf{b}}\mathbf{b}^{-1}\right| = \left|\mathbf{H}^{-1}\hat{\mathbf{H}}\right|,\ \ \mathbf{D} = 1{,}5 \cdot \mathbf{H}^{-1}\sum_{i \in P}\mathbf{J}_i^T\mathbf{F}_i\,, \tag{14}$$

where $\hat{\mathbf{H}}$ and $\hat{\mathbf{h}}_\mathbf{0}$ are calculated based on the known model taken from CAD and **H** and $\mathbf{h}_0$ based on another model with increased masses and moments of inertia which has been used as the real system, as will be explained in more detail in chapter 5.

It is shown in [15] that control law:

$$\boldsymbol{\tau} = \hat{\mathbf{b}}^{-1}(\mathbf{u_{eq}} - \mathbf{K}\,\mathrm{sgn}(\mathbf{s})) = \hat{\mathbf{H}}(\ddot{\mathbf{q}}_\mathbf{d} - \mathbf{K_1}\dot{\mathbf{e}} - \mathbf{K_0}\mathbf{e} - \mathbf{K}\,\mathrm{sgn}(\mathbf{s})) + \hat{\mathbf{h}}_\mathbf{0}\,, \tag{15}$$

with gain of discontinuous term **K** given with:

$$\mathbf{K} \geq \boldsymbol{\beta}(\mathbf{F} + \boldsymbol{\eta} + \mathbf{D}) + (\boldsymbol{\beta} - 1)\left|\mathbf{u}_{eq}\right|\,, \tag{16}$$

satisfies the sliding condition. $\hat{\mathbf{H}}$, $\hat{\mathbf{h}}_\mathbf{0}$ are calculated on basis of a known model. To eliminate chattering effect approximation of sign function in a thin boundary layer around **S** surface has been done. For this purpose proportional-integral combination of sliding function in boundary layer, given in [20] has been used. Saturated proportional-integral functions are introduced:

$$\rho(\sigma_i)=\begin{cases}1, & \sigma_i \le 1\\ \sigma_i + K_{Ii}\int_{t_{i0}}^{t_i}\sigma_i dt, & -1\le\sigma_i\le 1\\ -1, & \sigma_i \le 1\end{cases}, \tag{17}$$

$$\sigma_i = \frac{S_i}{\Phi_i},\ i=1,...,N\ , \tag{18}$$

where Φ is a thickness of a boundary layer, $K_{Ii}>0$ is integral gain and t_{i0} is the initial time when system states enter boundary layer [20]. Control law is now given in the form:

$$\boldsymbol{\tau} = \hat{\mathbf{H}}(\ddot{\mathbf{q}}_\mathbf{d} - \mathbf{K_1}\dot{\mathbf{e}} - \mathbf{K_0}\mathbf{e} - \mathbf{K}\boldsymbol{\rho}(\boldsymbol{\sigma})) + \hat{\mathbf{h}}_\mathbf{0}\ , \tag{19}$$

4.3. State and disturbance estimator

Feedback linearized system in presence of disturbance has the following form:

$$\ddot{\mathbf{q}} = \mathbf{v} + \mathbf{d}\ , \tag{20}$$

Extended state space model is defined:

$$\mathbf{x_1} = \mathbf{q}, \mathbf{x_2} = \dot{\mathbf{q}}, \mathbf{x_3} = \mathbf{d}\ , \tag{21}$$

$$\frac{d}{dt}\begin{bmatrix}\mathbf{x_1}\\ \mathbf{x_2}\\ \mathbf{x_3}\end{bmatrix} = \begin{bmatrix}0 & 1 & 0\\ 0 & 0 & 1\\ 0 & 0 & 0\end{bmatrix}\begin{bmatrix}\mathbf{x_1}\\ \mathbf{x_2}\\ \mathbf{x_3}\end{bmatrix} + \begin{bmatrix}0\\ 1\\ 0\end{bmatrix}\mathbf{v}\ , \tag{22}$$

$$\mathbf{y} = \mathbf{x_1} = \begin{bmatrix}1 & 0 & 0\end{bmatrix}\begin{bmatrix}\mathbf{x_1}\\ \mathbf{x_2}\\ \mathbf{x_3}\end{bmatrix}. \tag{23}$$

State space model of state and disturbance estimator is given with following expression:

$$\frac{d}{dt}\hat{\mathbf{X}} = \mathbf{A}\hat{\mathbf{X}} + \mathbf{B}\mathbf{v} + \mathbf{L}(\mathbf{y} - \mathbf{C}\hat{\mathbf{X}})\ , \tag{24}$$

$$\frac{d}{dt}\begin{bmatrix}\hat{\mathbf{q}}\\ \hat{\dot{\mathbf{q}}}\\ \hat{\mathbf{d}}\end{bmatrix} = \begin{bmatrix}0 & 1 & 0\\ 0 & 0 & 1\\ 0 & 0 & 0\end{bmatrix}\begin{bmatrix}\hat{\mathbf{q}}\\ \hat{\dot{\mathbf{q}}}\\ \hat{\mathbf{d}}\end{bmatrix} + \begin{bmatrix}0\\ 1\\ 0\end{bmatrix}\mathbf{v} + \begin{bmatrix}l_1\\ l_2\\ l_3\end{bmatrix}(\mathbf{q} - \hat{\mathbf{q}})\ , \tag{25}$$

where $\hat{\mathbf{q}}$ is a vector of estimated joint positions, $\hat{\dot{\mathbf{q}}}$ is a vector of estimated joint velocities, $\hat{\mathbf{d}}$ is the vector of estimated disturbances and $\mathbf{L}$ is vector of corrective factor gains. Poles of estimator are chosen to be four times faster than poles of process. Knowing values of these poles, corrective gains l_1, l_2 and l_3 are calculated using *acker* formula in MATLAB. Estimated disturbance acts as an integral term in control law and

eliminates the steady-state error. Integral anti-windup is implemented by restricting the derivative of estimated disturbance as follows:

$$\frac{d}{dt}\hat{\mathbf{d}} = \begin{cases} l_3(\mathbf{q}-\hat{\mathbf{q}}), \hat{\mathbf{d}} \in (d_{min}, d_{max}) \vee (\hat{\mathbf{d}} \geq d_{max} \wedge (\mathbf{q}-\hat{\mathbf{q}}) < 0) \vee (\hat{\mathbf{d}} \leq d_{min} \wedge (\mathbf{q}-\hat{\mathbf{q}}) > 0) \\ 0, \ (\hat{\mathbf{d}} \geq d_{max} \wedge (\mathbf{q}-\hat{\mathbf{q}}) > 0) \vee (\hat{\mathbf{d}} \leq d_{min} \wedge (\mathbf{q}-\hat{\mathbf{q}}) < 0) \end{cases}, \quad (26)$$

where d_{min} and d_{max} are allowed boundary values of disturbance which define the region where anti-windup is inactive. Sliding mode control law with disturbance estimator is now given with the following expression:

$$\boldsymbol{\tau} = \hat{\mathbf{H}}(\ddot{\mathbf{q}}_\mathbf{d} - \mathbf{K}_1\dot{\mathbf{e}} - \mathbf{K}_0\mathbf{e} - \mathbf{K}\boldsymbol{\rho}(\boldsymbol{\sigma}) - \hat{\mathbf{d}}) + \hat{\mathbf{h}}_\mathbf{0}. \quad (27)$$

5. Simulation Results

The efficiency of the proposed control algorithm, for simultaneous motion control of multi-segment lumbar spine and dual arm system, was tested through a numerical simulation. An example of manipulation task in presence of parameter uncertainties and external disturbances was simulated. The desired task for the robot was to pick up the object of unknown mass (yellow cube) from the table, move it to the side and drop it down on the ground. The simulation illustrates well how movable spine increases robot workspace and contributes to anthropomorphic look of robot motion. Stick diagram of simulated movement is shown in Fig.4. As it is shown in Fig. 4 at the beginning object is on the table and its weight is supported by the reaction force from the table. While the robot is carrying the object its weight is considered as an external disturbance to the system. In the initial pose trunk is in the upright position and left arm is about to grasp the object. In final posture, where robot drops the object, spine reaches its mechanical limit with total lateral flexion (30°) and rotation (45°) (as in right drawing in Fig. 2).

Mechanical parameters of the robot were taken from the CAD model. Such model is used for computation of $\hat{\mathbf{H}}$ and $\hat{\mathbf{h}}_\mathbf{0}$ in (27). In order to simulate parameter uncertainties, another model with same geometry but with increased masses and moments of inertia was used as a real system in simulation. In this model all segment masses are increased by 30% and all elements of inertia tensors by 20%.

Two external disturbances were introduced to the system in the simulation. First one came from the object weight, which was unknown to the robot, and it was simulated as the constant external force F_1=30 N (equivalent to the weight of 3 kg) acting on the left hand in negative direction of Z-axis. Second one was constant external force F_2=100 N acting along Y-axis on robot torso in the intersection of chest and spine. Both disturbances were generated as smooth Gaussian functions with a constant value in a specific time range. Disturbance F_1 started acting on the system at the moment when robot grasped the object t_1=0,2 s and stopped when robot dropped it on the ground at t_2=1,7 s. Disturbance F_2 had constant value in a time range between t_3=1 s and t_4=1,2 s. Simulation represents the situation when the robot upper-body is pushed from the side while carrying the object of unknown mass. Although the disturbance is constant force in global coordinates, it generates time-varying moments in robot joints.

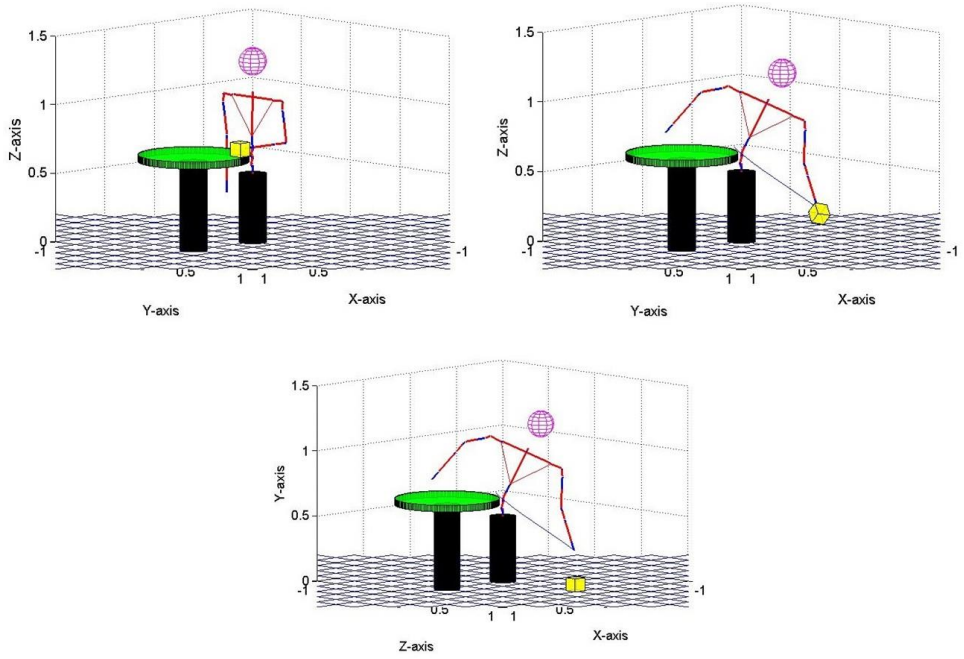

Fig. 4 Stick diagram of initial posture (upper left), middle phase (upper right) and final posture (down) of simulated motion

Fig. 5 shows input torques and time change of **S** hyper-surface for first (lateral flexion) and second (rotation) DOF of spine, from the base. These two DOFs are chosen as representative because they are most loaded. Simulation results have shown that proposed control algorithm provides chattering-free control input signals. This is very important because chattering effect can induce unmodeled high frequency dynamics which can lead to system instability. It can be seen from Fig. 5 that **S** surface converges to zero even in presence of disturbance, which means that the sliding condition is achieved. Small peaks can be noticed on graphs of input torques at time instants in which external disturbance starts and stops acting on the system (1 s; 1,2 s; 1,7 s). In Fig. 6 input torques and dynamics of **S** surface for shoulder flexion and elbow flexion joint are shown.

It can be seen from Fig. 6 that **S** surface for arm joints also converges to zero, which means that tracking error converges to zero. All joints in robot upper-body are coupled and influenced by external disturbances. Small positioning error in spine joints can cause significant error of gripper position in global coordinate frame, so it is very important to achieve accurate trajectory tracking.

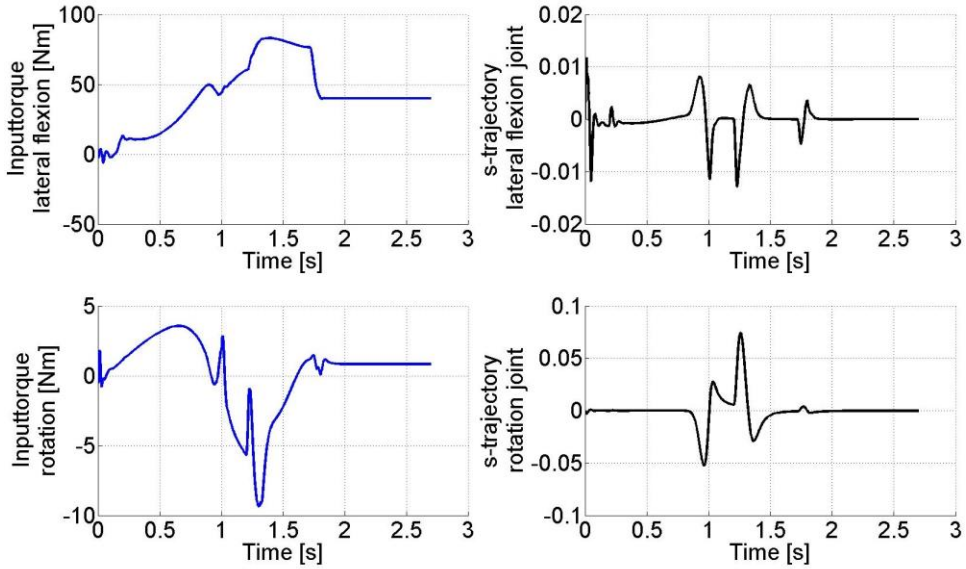

Fig. 5 Chattering-free input torques (left) and s-trajectories (right) for spine lateral flexion joint and rotation joint

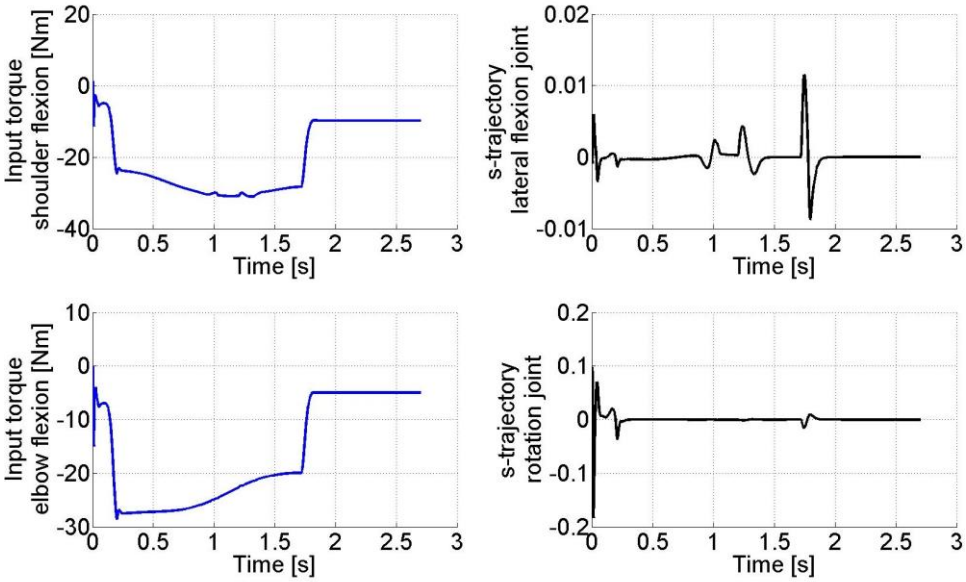

Fig. 6 Chattering-free input torques (left) and s-trajectories (right) for left shoulder flexion joint and elbow flexion joint

Fig. 7 shows position error of the point where neck intersects with clavicles, measured in global coordinate frame while Fig. 8 shows positioning error of the left hand.

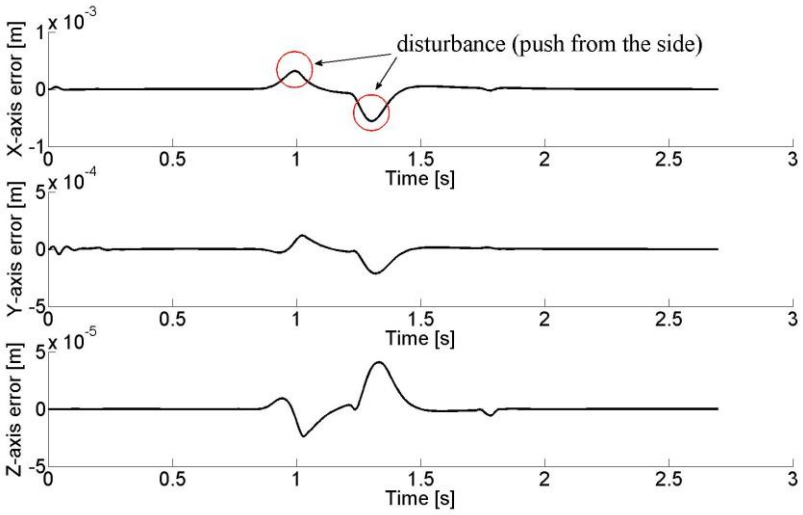

Fig. 7 Position error of intersection point of neck and clavicles in global coordinate system

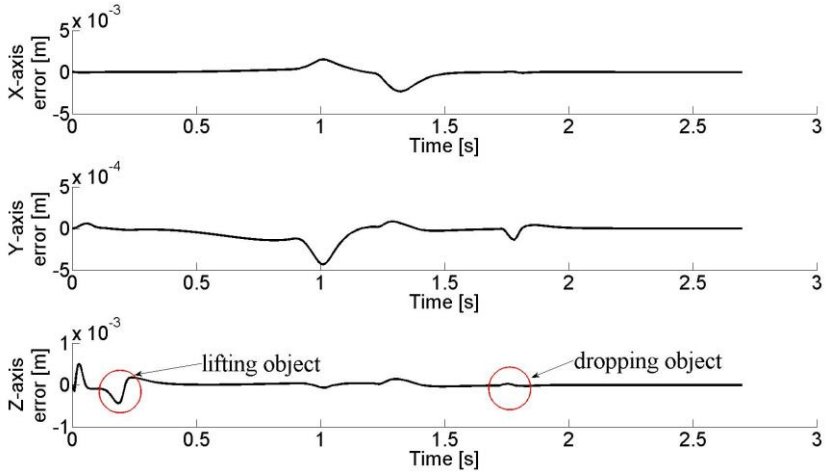

Fig. 8 Position error of the left hand in global coordinate system

It can be seen from Fig. 7 that maximal value of position error is less than 1mm on a whole trajectory. This result confirms that proposed control law is robust to significant parameter uncertainties and has ability of disturbance compensation.

Trajectory synthesis was done in joint space, based on desired initial and final joint positions and maximum allowed values for angular velocities and accelerations. All joint trajectories in simulation were computed offline using seventh order polynomials. This

way smooth function for angular positions, velocities, accelerations and jerks were obtained. Trajectories consist of two phases. In the first phase each joint tracks a predefined trajectory from initial to final state, and in the second phase robot holds final position for additional second.

6. CONCLUSION

In this paper mechanical design of humanoid robot upper-body, consisting of two arms and lumbar spine, was presented and robust nonlinear control algorithm was proposed. Presented control law is a combination of feedback linearization and sliding mode control with implemented state and disturbance estimator. Anti-chattering technique based on constant thickness boundary layer has been implemented. Efficiency of the proposed algorithm was tested through a numerical simulation. Task, which includes simultaneous motion of robot spine and arms and manipulation with an object of unknown mass in presence of external disturbance, has been simulated. Results show that proposed control law achieves great tracking accuracy and successfully deals with parameter uncertainties and compensates for disturbances. Biologically inspired mechanical design provides operating range and functionality similar to humans. Presented multi-segment lumbar spine increases workspace of robot arms and contributes to natural appearance of motion. In further work, an additional joint will be added in a spine base to allow flexion and extension of the robot spine. Models of actuators and gears with actuator saturations will be also included in the overall dynamic model to make it more realistic. Support vector regression will be considered as a possible solution for learning inverse dynamics for manipulation tasks.

REFERENCES

[1] ABB, Dual-arm concept robot, 2014. [Online]. Available: http://www.abb.com/cawp/abbzh254/8657f5e05ede6ac5c1257861002c8ed2.aspx [Access on March 2014].

[2] A. Albers, S. Brudniok, J. Ottnad, "ARMAR III-design of the upper body," in *Proceedings of 6th International Conference on Humanoid Robots*, *IEEE-RAS*, Genova, Italy, pp. 308−313, 2006. [Online]. Available: http://www.sfb588.uni-karlsruhe.de/old/publikationen/2006/R5_Albers_HCRS06.pdf

[3] E. Wade, A. Parnandi, R. Mead, M. Matarić, "Socially assistive robotics for guiding motor task practice," PALADYN Journal of Behavioral Robotics, vol. 2, no. 4, pp. 218−227, 2011. [Online]. Available: http://robotics.usc.edu/publications/media/uploads/pubs/764.Paladyn.2.2011.pdf

[4] H. Iwata, S. Sugano, "Design of human symbiotic robot TWENDY-ONE," in *Proceedings of IEEE International Conference on Robotics and Automation 2009*, *ICRA 2009*, Kobe, Japan, pp. 580−586, 2009. [Online]. Available: http://dx.doi.org/10.1109/ROBOT.2009.5152702

[5] J. Tasevski, M. Nikolić, D. Mišković, "Integration of an industrial robot with the system for image and voice recognition," Serbian Journal of Electrical Engineering, vol. 10, no. 1, pp. 219−230, 2013. [Online]. Available: http://www.doiserbia.nb.rs/img/doi/1451-4869/2013/1451-48691301219T.pdf

[6] O. Eiberger, W. Friedl, B. Baüml, G. Hirzinger, "A humanoid two-arm system for dexterous manipulation," in *Proceedings of 6th International Conference on Humanoid Robots*, *IEEE-RAS*, Genova, Italy, pp. 276−283, 2006. [Online]. Available: http://dx.doi.org/10.1109/ICHR.2006.321397

[7] M. A. Diftler, R. O. Ambrose, S. M. Goza, K. S. Tyree, E. L. Huber, "Robonaut mobile autonomy: Initial experiments," in *Proceedings of IEEE International Conference on Robotics and Automation 2005*, *ICRA 2005*, Barcelona, Spain, pp. 1437−1442, 2005. [Online]. Available: http://dx.doi.org/10.1109/ROBOT.2005.1570315

[8] I. Boblan, A. Shulz, "A humanoid muscle robot torso with biologically inspired construction," in *Proceedings. of 41st International Symposium on Robotics (ISR) and 6th German Conference on Robotics (ROBOTIK)*, Munich, Germany, pp. 1−6, 2010.

[9] I. Mizuuchi, R. Tajima, T. Yoshikai, D. Sato, K. Nagashima, M. Inaba, Y. Kuniyoshi, H. Inoue, "The design and control of the flexible spine of a fully Tendon-Driven humanoid Kenta," in *Proceedings of International Conference on Intelligent Robots and Systems*, *IEEE/RSJ 2002*, Lausanne, Switzerland, pp. 2527–2532, 2002. [Online]. Available: http://dx.doi.org/10.1109/IRDS.2002.1041649

[10] I. Mizuuchi, M. Inaba, H. Inoue, "A flexible spine human-form robot – Development and control of the posture of the spine," in *Proceedings of International Conference on Intelligent Robots and Systems*, *IEEE/RSJ 2001*, Maui, Hawaii, pp. 2099–2104, 2001. [Online]. Available: http://dx.doi.org/10.1109/IROS.2001.976381

[11] I. Mizuuchi, T. Yoshikai, Y. Sodeyama, Y. Nakanishi, A. Miyadere, T. Yamamoto, T. Niemela, M. Hayashi, J. Urata, Y. Namiki, T. Nishino, M. Inaba, "Development of musculoskeletal humanoid Kotaro," in *Proceedings of IEEE International Conference on Robotics and Automation*, *ICRA 2006*, Orlando, Florida, pp. 82–87, 2006. [Online]. Available: http://dx.doi.org/10.1109/ROBOT.2006.1641165

[12] W. M. Hinojosa, N. G. Tsagarakis, G. Metta, F. Becchi, G. Sandini, D. G. Caldwell, "Performance assessment of a 3 DOF differential based waist joint for the "iCub" baby humanoid robot," in *Proceedings of 15th IEEE International Symposium on Robot and Human Interactive Communication*, *RO-MAN 2006*, Hatfield, pp. 195−201, 2006. [Online]. Available: http://dx.doi.org/10.1109/ROMAN.2006.314417

[13] C. Sander, T. Soworka, A. Albers, "Design of a new torso-joint for the humanoid robot ARMAR," Journal of Mechanical Engineering and Automation, vol. 2, no. 4, pp. 58−64, 2012. [Online]. Available: http://article.sapub.org/pdf/10.5923.j.jmea.20120204.02.pdf

[14] M. Penčić, "Lumbar spine development for humanoid robots," Zbornik radova Fakulteta tehničkih nauka, vol. 27, no. 14, pp. 3091−3094, 2012 (in Serbian).

[15] J. E. Slotine, W. Li, *Applied Nonlinear Control*, Prentice Hall, Englewood Cliffs, New Jersey, 1991.

[16] K. D. Young, V. I. Utkin, Ü. Ozgüner, "A control engineers guide to sliding mode control," IEEE Transactions on Control System Technology, vol. 7, no. 3, pp. 328−342, 1999. [Online]. Available: http://www.diee.unica.it/~eusai/BOSIO/%5B4%5D%20%20A_control_engineers_guide%20to%20SMC.pdf

[17] D. Krklješ, M. Nikolić, S. Savić, L. Nađ, K. Babković, "Humanoid robot wrist prototype," in *Proceedings of 48th International Conference on Microelectronics, Devices and Materials*, *MIDEM*, Otočec, Slovenia, pp. 255−260, 2012.

[18] S. Savić, M. Jurošević, "Design of an anthropomorphic robot arm," in *Proceedings of 56th ETRAN*, Zlatibor, Serbia, pp.1−4, 2012 (in Serbian).

[19] V. Potkonjak, M. Vukobratović, K. Babković, B. Borovac, "General model of dynamics of human and humanoid motion: feasibility, potentials and verification," International Journal of Humanoid Robotics, vol. 3, no. 2, pp. 21−48, 2006. [Online]. Available: http://dx.doi.org/10.1142/S0219843606000679

[20] T. V. M. Nguyen, Q. P. Ha, H. T. Nguyen, "A chattering-free variable structure controller for tracking of robotic manipulators," in *Proceedings of the Australasian Conference on Robotics and Automation*, *ACRA 2003*, Brisbane, Australia, pp. 1−6, 2003. [Online]. Available: http://epress.lib.uts.edu.au/research/bitstream/handle/10453/7241/2003001213.pdf?sequence=1